MYRRHA: Design and Verification Experiments for the Windowless Spallation Target of the ADS Prototype MYRRHA

Katrien Van Tichelen, Peter Kupschus, Hamid Aït Abderrahim
SCK•CEN
Boeretang 200, B-2400 Mol, Belgium
myrrha@sckcen.be

Dr. A. Klujkin, Dr. E. Platacis
Institute of Physics, University of Latvia
Salaspils-1, Miera str. 32, LV-2169 Latvia

Abstract – *SCK•CEN, the Belgian Nuclear Research Centre, works on the conceptual design and basic engineering of a multipurpose ADS for R&D, dubbed MYRRHA, a small high-performance irradiation facility with fast neutron fluxes up to 1.10^{15} $n/cm^2/s$ to start operation in about 2010. It is to serve for demonstrating the ADS concept and to be used for research on structural materials and nuclear fuel, liquid metals and associated aspects, reactor physics and subsequently on applications such as waste transmutation, radioisotope production and safety of sub-critical systems.*

In (Van Tichelen, 2000) the basic arguments for the windowless design of the spallation source at the centre of the sub-critical core (SC) have been outlined. Revised requirements have resulted in the upgrading of the primary proton source to 350 MeV and 5 mA. Accordingly, the spallation source will now have to absorb 1.75 MW from the beam, penetrating into a volume of lead/bismuth eutectic flow to a depth of about 13 cm. About 80% of this power stay in the liquid metal in the form of heat to be carried away at a flow rate of 10 l/s. The target is formed by a co-axial confluence in a loop that is now open rather than coaxial, because of the space limitations imposed by the high-performance SC. Because the free surface at the confluence is not the highest point in the (mainly vertical) loop the flow from the upper annular channel has to be drag limited. The minimisation and enhancement of heat transfer of the re-circulation zone close to the free surface guide the optimisation of the confluence flow pattern.

Further to (Van Tichelen, 2000), the design verification experiments – at the time being performed with water under ambient air pressure – have been conducted at IPUL in a mercury loop whose size with a contents of 8 ton Hg presents an even match to the later MYRRHA loop. This loop has also been made to operate under vacuum in order to comply with the later requirements and to avoid the entrainment of air. The first indications are that the quality of the produced free surface at the desired flow rate does match the formerly reported one in the water experiments in similar conditions. Moreover, the envisaged optimisation path to obtain a minimum re-circulation zone has proven to work. This completely closed circuit of proper magnitude has as a by-product shown a number of systems properties the knowledge of which will be very valuable in the proper design of the MYRRHA loop. Three different kinds of nozzles with varying parameter details are being investigated. The circuit, the experiments and the results obtained so far will be reported.

I. INTRODUCTION

At the heart of an Accelerator Driven System is the spallation target. It is the neutron source providing primary neutrons that are multiplied or amplified by the surrounding subcritical core (SC). The primary neutrons are produced by the spallation reaction of heavy target nuclei under impinging high-energy protons generated by a suitable particle accelerator. The amount of spallation neutrons depends on the initial energy of the incident particle and on the atomic number of the target nuclei. For instance, for a lead target bombarded with 350 MeV protons one expects a yield of 6 n/p (thick target, Aït Abderrahim, 2001) and for the Pb-Bi eutectic liquid metal (LM) the same yield is expected.

Due to the high Z efficiency, a heavy metal is the most appropriate solution for the target. Moreover, due to very high power density one arrives at due to space limitations when optimising the subcritical core performance, a liquid metal remains the only option permitting to remove the heat by forced convection.

The MYRRHA subcritical core consists of hexagonal assemblies of MOX Fast Reactor-type fuel pins with an active length of 600 mm placed centrally in a LM pool (Aït Abderrahim, 2000/2001). Two configurations - that are different with respect to the size of the hexagon – are currently studied. In the 'large assembly'-configuration, one single central hexagon is removed. In the small assembly configuration, three central hexagons are removed. This is shown in Fig. 1. Both configurations leave a gap around the spallation target's flow return tube (of 72 mm ID, 80 mm OD) – being filled with the SC liquid Pb-Bi coolant. The outside dimensions of this gap are constrained by the neutronic performances of the core: in order to obtain the required fast neutron fluxes for high flux irradiation samples to be placed in this gap – e.g. for minor actinide transmutation investigations - the gap width is restricted to the dimensions shown in Fig. 1 (Malambu, 2000). Above the axial region of the spallation source – which, with its ca 13 cm axial length, is centrally placed in the SC's 60 cm active length - the feeder downcomer and a nozzle, taking the liquid to the centre position, can use the full space created by removing the above hexagon(s). It is clear that in the 'small assembly'-configuration the feeder section is more difficult. For the moment, the investigations have been focussed on the 'large assembly' case. The position of the target in MYRRHA is shown in Fig. 2 in plan view.

Large assemblies   Small assemblies
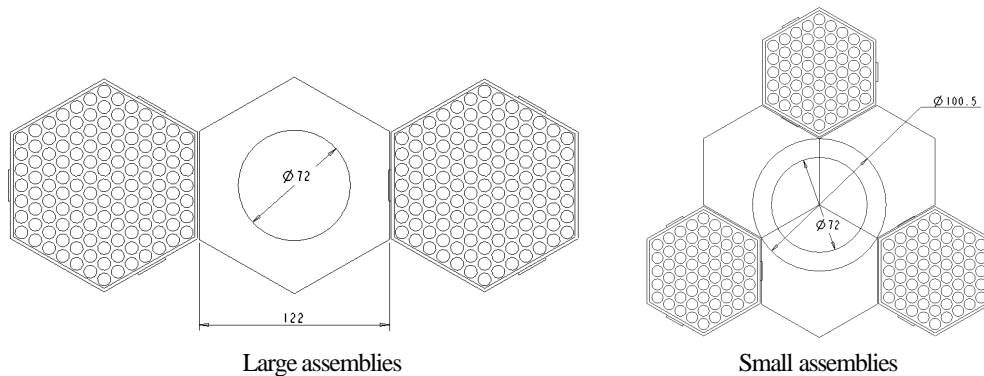
Figure 1. Dimension of the central gap for the spallation target in the hexagonal core of MYRRHA

With the above space limitations it is intended to deliver the 5 mA protons in form of a pencil beam scanning the available surface in side the 72 mm ID in such a way that it best matches the re-circulation pattern of the free surface and according provisions are foreseen in the ion optics of the accelerator. Apart from the space limitations and material property short-comings, also the current and power density figures would make the design of a solid window for the spallation source next to impossible: the chosen 5 mA at the relative low energy leads to a current density of order 150 µA/cm^2 (as far as we know at least a factor of 3 higher than any window design that has been attempted to meet). This is the main reason for adopting the windowless design for MYRRHA which has as a consequence that the free surface ultimately has to be compatible with the vacuum requirements of the beam transport system of the accelerator. The total beam energy will be dumped into a volume of ca 0.5 l leading to a heating power density of ca 3 kW/cm^3. In order to remove this heat from the LM with an average temperature increase of 150°C on top of the temperature of the inlet flow of 200°C a total flow rate of 10 l/s at an average flow speed of 2.5 m/s is required. It is suggested from estimates that the evaporation from 'hot spots' with elevated temperatures beyond the average 350°C - close to the free surface in the re-circulation zone (and these are the only ones of interest for the vacuum compatibility problem) – is then still acceptable. The investigation is therefore directed to assess and minimise the re-circulation zone inherent in the free surface formation under the above geometry and flow requirements.

To summarise, the challenge in the MYRRHA spallation target design is to create a Pb-Bi flow pattern with a free surface within the geometrical constraints, adequate to remove the heat deposited by the proton beam so that the thermal and vacuum requirements are met.
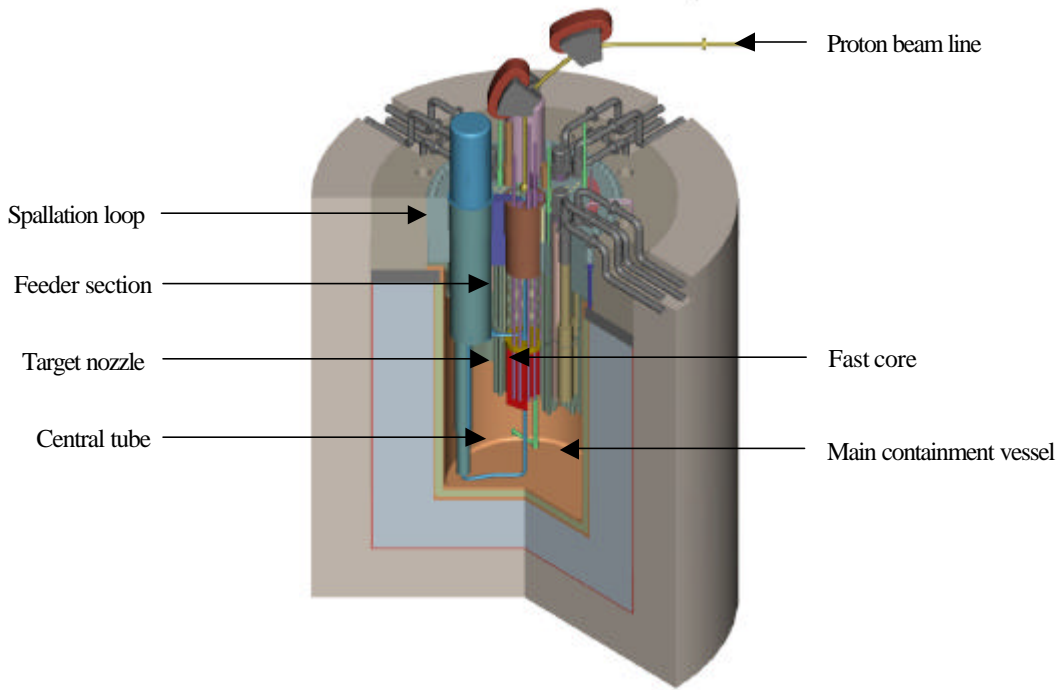
Figure 2. The position of the spallation target in the MYRRHA system

II. DESIGN PROGRAM

To gain insight in the characteristics and expertise in the creation of an adequate free surface flow, SCK•CEN has developed a roadmap of experiments with increasing correspondence to the real situation. This roadmap is supported and guided by Computational Fluid Dynamic (CFD) calculations. The CFD calculations are also used to investigate the flow pattern and temperature profile in the presence of beam heating which cannot be simulated experimentally at this stage.

I. Dimensionless Analysis

Since to-scale experiments with Pb-Bi eutectic LM are more difficult to conduct due to its high melting temperature, water and mercury are used as simulating fluids in the first and second instance. It can be seen from the analysis of the relevant dimensionless numbers that these fluids are suitable for simulating the LM hydraulics.

A free surface flow under gravity in which surface tension might play an important role, is determined by the dimensionless numbers Reynolds, Froude and Weber:

$$Re = \frac{\rho V D_h}{\mu} \qquad Fr = \frac{V}{\sqrt{g D_h}} \qquad We = \frac{\rho V^2 D_h}{\sigma} \qquad (1)$$

Herein is :
ρ   the fluid density,
μ   the fluid dynamic viscosity,
σ   the fluid surface tension,
V   the fluid velocity,
D_h a characteristic length and
g   the gravity constant.

Comparing these numbers for the relevant velocity (v = 2.5 m/s) and characteristic length (D_h = 72 mm = central tube diameter) at a relevant temperature, leads to the result shown in Table 1.

	T (°C)	Re	Fr	We	Pr
Pb-Bi	200	7.28E+05	8.54	13013	0.032
H$_2$O	20	1.77E+05	8.54	5966	6.890
Hg	20	1.55E+06	8.54	15694	0.027

Table 1. Dimensionless numbers

It can be seen that for all three liquids, the Reynolds numbers for the central tube are clearly in the turbulent flow range; this is also true for the annular gap of the downcomer. The Reynolds number for Pb-Bi is between the water and Hg values. The Froude number is equal in all cases since velocity and characteristic length are specified. The Weber similarity is also acceptable. Again, the Pb-Bi value is between the water and Hg values. Therefore, it was concluded that water and mercury are suitable fluids for simulating the Pb-Bi flow behaviour. Pb-Bi lies within the span of the two liquids. In view of this, the optimisation of nozzles can be done using the relatively easy-to-handle water and mercury and confirmation experiments have to be carried out using Pb-Bi.

As can be seen from the Prandtl number that describes the heath transfer capability of the liquids, LM experiments remain indispensable for analysing the thermal aspects.

II. Water Experiments at UCL

In June 1999 an R&D program started in collaboration with the thermal-hydraulics department of Université Catholique Louvain-la-Neuve (UCL, Belgium), in short TERM. Within this R&D program, water experiments on a one-to-one scale under atmospheric pressure were performed. As stated above, water was used because of its ease of handling. Due to equipment limitations at the time and the initial lower specification of the beam specifications, most experiments were performed at a nominal flow rate of 5 l/s leading to an average flow speed of 1.3 m/s, only a few at close to 7 l/s.

As result of the experimental investigations (Van Tichelen, 2000 and Seynhaeve, 2000), a stable free surface at different fluid levels could be established. The experiments showed the necessity of taking provisions to suppress possible swirl creation in the central tube originating from the feeder section. The experimental nozzle and the resulting free surface are shown in Fig. 3. Also shown is a comparison between LASER Doppler Velocimetry (LDV) measurements of the velocities in the entrance region and the output of CFD calculations.

In the centre where the down coming flow meets, a so-called re-circulation zone or 'hydraulic jump' is formed. In this zone, the stream lines are forming a closed cell torus in which the velocity direction is vertically upwards along the central axis (negative velocities in LDV and CFD up to –0.4 m/s), flows radially outwards and returns parallel with the main flow streamlines (positive velocities up to 1 m/s).

Figure 3. The nozzle in the water target experiment

Experiments introducing dye in the flow have shown that the residence time of fluid particles in the re-circulation zone is on the brink of being critical. This has important implications on the fluid temperatures at the free surface when the beam heating will be present. The longer the residence times, the higher the temperature and the higher the vaporisation of the LM into the beam line. Minimising the residence times by minimising the re-circulation zone is seen as a major tool to handle the surface heating.

The water experiments did not allow this optimisation as at a certain minimisation level air from the atmosphere above is entrained in the flow leading to two-phase conditions with entirely different flow properties. This limited the usefulness of the water experiments under atmospheric pressure, however, some confidence was taken from the co-incidence of the experimental and CFD flow field evaluation in the re-circulation region.

III. Hg Experiments at IPUL

To eliminate the possibility of air entrainment and to step forward in the approach towards the assessment, a to-scale experiment using liquid Hg at a flow rate of 10 l/s and under adequate vacuum conditions has been conceived by SCK•CEN and carried out at the Institute of Physics (IPUL) of the University of Latvia in Riga, Latvia. A drawing of the target module is shown in Fig. 4. This module houses the different nozzles that are tested and is placed into the existing Hg loop at IPUL. All experiments are performed in collaboration with IPUL.
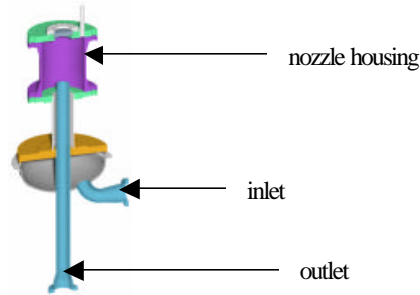
Figure 4. The target module in the Hg experiment

I. Description of the Experimental Loop

The experimental loop (shown in Fig. 5) at IPUL contains 8 ton of liquid mercury and is in this way an even match to the later MYRRHA loop. Its main parts are an MHD pump, a loop main valve, a heat exchanger to remove the pump heat losses to the mercury, a test section and an MHD flow meter. The MYRRHA module is inserted in the test section.

To remove or add small amounts of mercury from or to the otherwise closed loop, a cylinder was installed and connected to the loop through a feeding line with a valve at the outlet of the module and a bleeding line with a valve at the inlet of the nozzle.

A vacuum system was added to the loop at the top of the module to establish vacuum above the free surface – typically to less than 0.1 mbar. This system also contains a whole circuit for proper de-airing of the loop at the start-up as it turned out during the first experiments that insufficient removal of air from the loop can cause an early onset of cavitation in certain cases.

Other possible sources of cavitation in the loop such as abrupt changes in cross-section were eliminated or reduced where possible. It is important to stress here that by using the term 'cavitation' we mean strictly the phenomenon of the LM flow detaching from the wall (with subsequent re-impingement onto the wall); we do not at this stage combine this in any way with the surface-corrosive action of cavitation as seen in a number of other technological areas.
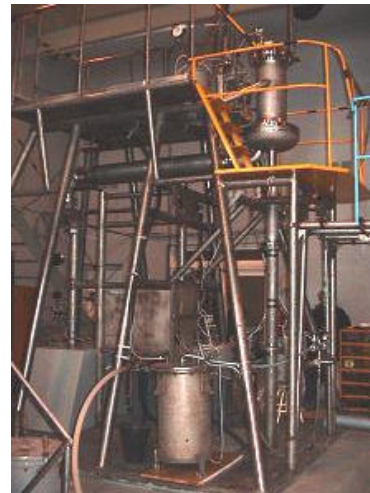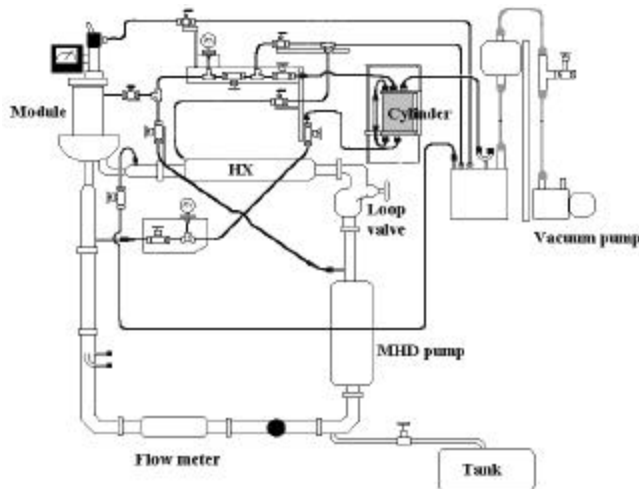
Figure 5. Hg experimental loop at IPUL, Latvia

During the experiments it became clear that the MHD pump needs a minimal pump load. At low loop resistance, the characteristics of MHD pump current I versus flow rate $\dot{V}$ show a kink that is likely due to cavitation within the MHD pump. Therefore, the loop valve was partially closed during the subsequent experiments in order to provide a minimum head/load to the pump. The above curve then becomes a straight line except for very low flow rates.

II. Small Gap Nozzle

The nozzle tested at UCL gave a lot of useful information but could never be used in the final spallation loop. The free surface of spallation is in the real situation not the lowest point in the loop. Therefore, the flow through the nozzle feeder should be drag limited in order to prevent the fluid from falling down. The gap of the feeder of the UCL nozzle is 20 mm and this is too wide to prevent the acceleration and finally tearing off of the liquid. As the feeder section in the UCL was relatively short, this did not influence the experiments. In reality, the feeder section will be of the order of 2 m and the liquid would fall down. Calculations have shown that for a gap of 5 mm width, the drag is sufficient to prevent the fluid from accelerating. Therefore, this gap width was chosen for the first Riga nozzle.

To maximise the useful space for irradiation samples, a sharp entrance angle into the central tube is most favourable. In this way, the samples can be positioned close to the highest flux region. An entrance angle of 33.0° was chosen for the first nozzle SG33.0 shown in Fig. 6.
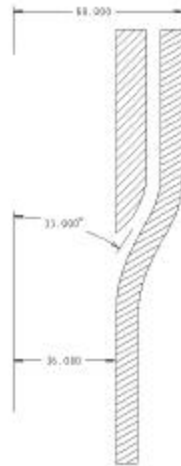
Figure 6. Nozzle SG33.0

The experiments showed a significant difference between the flow for the nozzle SG33.0 and the UCL nozzle in three respects:

- The reduced gap leads to large difference between the velocity in the feeder and in the central tube, whereas in the IPUL nozzle their ratio was almost 1. This mismatch (close to factor 3) in the present conception leads to a much 'noisier' free surface.
- This noisier free surface sheds a small droplet spray much easier than water and this would be unacceptable for the target use because the droplets will be vaporised during their lifetime that is of order fraction of a second.
- Full through-put to 10 l/s could not be reached because of the occurrence of frighteningly noisy cavitation in parts of the loop (quite different from the water experience) predominantly at the diffuser like widening of the loop cross section in the SCK·CEN module after the target section.

With respect to the first point, it was decided to design a second nozzle with a larger feeder cross-section in order to eliminate the velocity mismatch, but to insert an intermediate septum to keep the drag limitation (see § II.). It was expected that also the problem of the droplet spray would vanish with these adaptations as the flow would become calmer.

With respect to the third point, different possible causes or influencing parameters for cavitation were identified. Proper de-aeration of the loop was made possible through a vacuum circuit and adaptations were made to the diffuser.
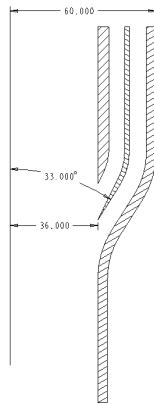
Figure 7. Nozzle DG33.0

III. Double Gap Nozzle

As already stated, the second nozzle for the mercury experiments has a double gap feeder which eliminates the velocity mismatch with the central tube while keeping the drag limitation. The entrance angle is kept the same. This nozzle is called DG33.0 and is shown in Figure 7.

A first campaign with this nozzle showed that the measures taken with respect to the cavitation problem have a positive influence. The cavitation - as measured in relative terms on a number of relevant places by accelerometers - was much reduced and a flow rate of 10 l/s could now be achieved. However, in most of the cases cavitation was still present.

Different runs with different initial (i.e. at 0 l/s) mercury levels showed the onset of cavitation at different flow rates. This is shown in Fig. 8. The left figure shows the level of vibration – the relative indication of the extent of cavitation - measured by a sensor attached to the module for different initial levels. The right figure gives the pressure at the outlet of the module (not corrected for the manometer height). For Run 4 the initial level is 14 cm above the nozzle entrance to the central tube (i.e. end point of the nozzle inner cylinder). For Runs 5, 6 and 7 the initial level is respectively about 20 cm, 18 cm and 19.8 cm above the inner cylinder end point. The observations during these runs are the following:

→ Run 4: Cavitation gradually sets in and reached a high level at high flow rates. Vibration levels become very high and increase with the flow rate in a more than quadratic way. The pressure at the outlet of the module goes to – 1 bar which corresponds to vacuum and indicates the presence of cavitation = detachment in this point. As the pressure reading indicates that cavitation takes place at the wall of the central tube following downward from the nozzle, we expected that one should be able to influence the level of cavitation by 'backfilling' this central tube. This would take the point

where the cavitation region re-collapses up and would reduce the level of cavitation. Therefore, Hg was injected from the cylinder through the lower pressure tap at 9 l/s. The expected effect occurred! The cavitation decreased and finally disappeared completely and the pressure reading recovered. Next, the cylinder was filled again and thus mercury was taken from the loop through the upper tap. In the first instance, the vibration level stayed at low values and the free surface level decreased. Only when the cylinder was nearly completely filled again, the vibration level began to rise up to high values and the free surface level did not decrease anymore.

→ Run 5: The vibration stays at a low level and the pressure remains positive. No cavitation occurs up to 11 l/s. At 9 l/s the cylinder was filled. Cavitation seemed not to set in, even until the cylinder was almost completely filled. The free level surface level decreased but the test had to be stopped as the cylinder was completely filled.

→ Run 6: For this run with an intermediate level, no cavitation could be heard up to a flow rate of 9 l/s. From then on, cavitation occurred but disappeared when the flow rate was reduced again. No mercury was taken from or fed to the loop.

→ Run 7: At 9 l/s the cylinder was filled through the upper pressure tap. The behaviour was similar to the Run 5, except that for high cylinder filling levels, cavitation sets in.

These experiments seemed to indicate that high starting levels might lead to nearly cavitation free runs, even when mercury is later on removed from the loop to the cylinder and the free surface level goes down. The desired very low surface level could not be established however as the volume of the present cylinder was to small to remove the sufficient amounts of Hg.
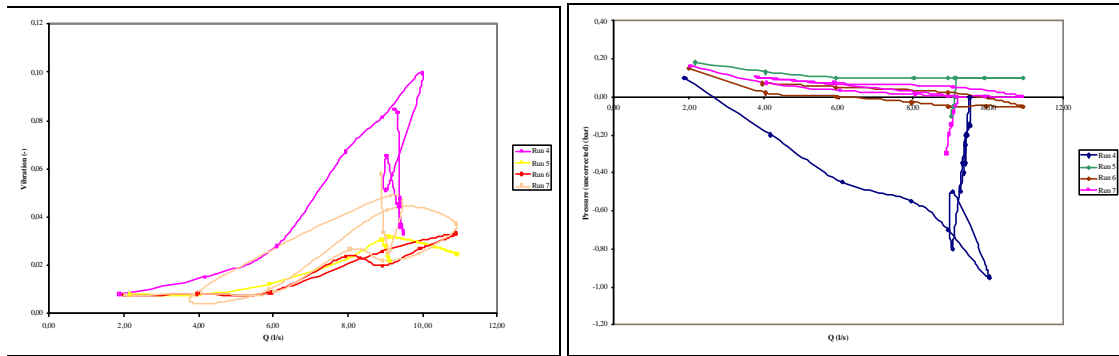
Figure 8. Dependence of cavitation onset on the initial level and the effect of backfilling

A second campaign was carried out in which the volume of the cylinder was doubled to allow further removal of Hg from the loop. Fig. 9 shows the results of a run with an initial level at 20 cm above the end point. The flow rate is set at 9 l/s. The aim was to investigate whether the free surface level could be further reduced by taking more Hg into the larger cylinder.

Fig. 9 shows at the right the level of the mercury in the nozzle and the cylinder measured with a newly installed resistance level probes (where 0 mm corresponds to the nozzle inner cylinder end point) and at the left the pressure at the inlet of the nozzle and at the diffuser (i.e. the module outlet) measured with new electrical manometers. It is to be said that while Hg is removed from the loop to the cylinder, the nozzle manometer measured an almost zero value as the manometer is installed in the draining line of the loop. While the Hg is added to the loop from the cylinder, the diffuser manometer shows more or less the static pressure of the Hg in the cylinder as this manometer is installed in the filling line. When the actions - removing or adding - are interrupted by closing the valves, the pressure values recover. This causes the peaks in the pressure curves.

In the first instance, the removal of Hg to the cylinder has an influence on the nozzle level. During this first period, no cavitation could be heard. At a certain time, cavitation sets in. This can be seen from the decrease of the diffuser pressure. From this moment on, the removal of Hg has no influence on the nozzle level. One clearly sees that although there is a significant change in the cylinder level, the nozzle level stays more or less constant. The cross-section of the nozzle and the cylinder are of the same order of magnitude, so, if the Hg that is filled to the cylinder would come from the nozzle, there should have been a significant change in the nozzle level too! As this is not the case, the Hg should come from somewhere else and most likely, the Hg is removed from the "cavitation" region.

When adding Hg from the cylinder to the loop, the nozzle level is only slightly influenced. However, the level of vibration is significantly reduced. The Hg added to the loop, most likely back-fills (i.e. reduces the void at) the cavitation region. This can be seen from Fig. 9 (bottom) showing the multi-meter value of a newly installed accelerometer at the module outlet.

These experiments clearly showed that this nozzle creates a flow with a large Hg dome at the free surface region that can be supported by the large radial velocities at the entrance of the free surface region. One is not able to influence the height of the dome through the removal of Hg from the loop as soon as cavitation sets in. The Hg is removed from the cavitation region.

In order to overcome this difficulty, the new, more slender nozzle was conceived and fabricated at IPUL. The entrance angle was reduced to 16.5°. CFD calculations have indicated that at this angle (see § II.IV.), cavitation free flow is possible. They also predict the possibility to position the free surface almost at liberty.

IV. Double Gap Nozzle with Smooth Entrance

The previous experiments showed that it was necessary to reduce high inward radial acceleration and velocity of the flow in the entrance region in order to reduce cavitation and to be able to reduce the large Hg dome. This is done by reducing the entrance angle of the nozzle from 33.0° to 16.5°. The double gap is still present. Therefore, this nozzle was called DG16.5 and is shown in Fig. 10.
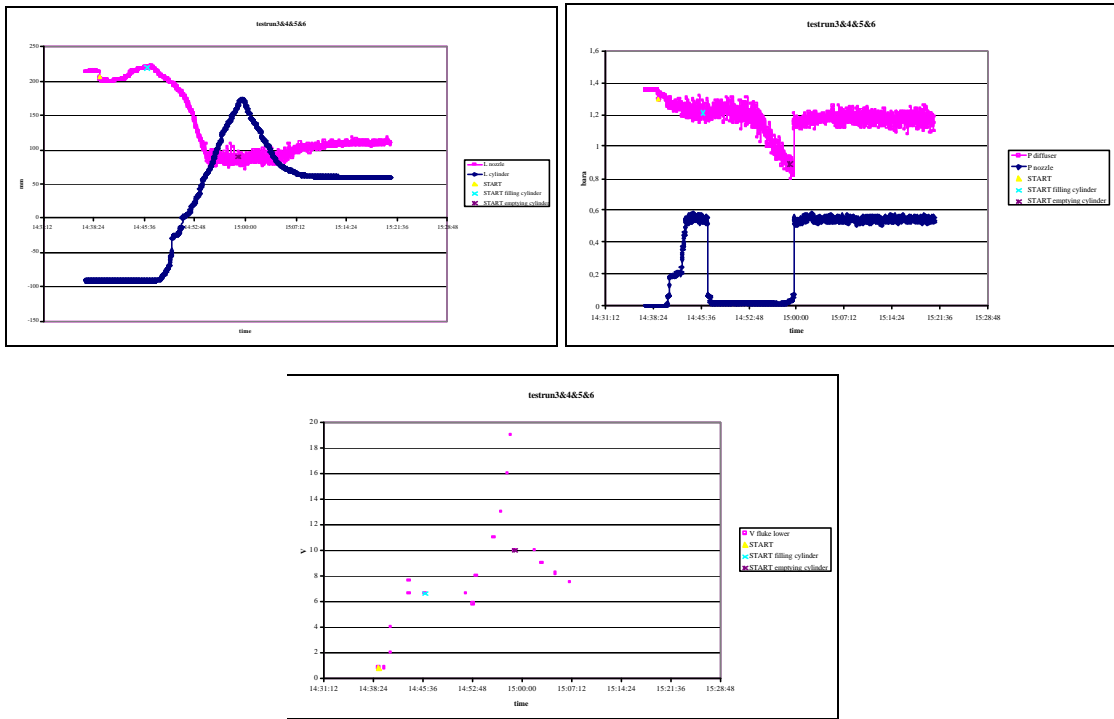
Figure 9. Effects of adding and removing Hg to and from the loop on Hg levels, pressures and vibrations
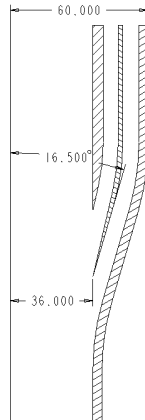
Figure 10. Nozzle DG33.0

The initial Hg level was set at 20 cm above the lowest point of the inner nozzle cylinder. The flow rate was set to 10 l/s. At this flow rate and Hg content of the loop, a relatively high free surface position was established. By removing Hg to the cylinder, the surface could be lowered and now as far as we wanted. The free surface did not stall at a certain level. As, cavitation was never present, mercury removed from the loop was taken from the free surface dome! Fig. 11 shows on the left a picture of the surface in an intermediate position. The conical shaped main flow at ~ 2.5 m/s and the re-circulation region can clearly be seen. In the middle, a picture of the surface at a lower position is shown where the re-circulation region had disappeared completely and a V-shaped free surface was obtained. In this lowest free surface position, significant spitting of Hg droplets from the surface was present. This is of course to be avoided. The loop was then filled again. At the level shown in the right picture of Fig. 11, the spitting disappeared almost completely.

The level of Hg in the cylinder is shown in Fig. 12. The nozzle level meter was removed because of mounting problems and not to obstruct the free surface formation. At 10 l/s, pressures were always positive, as can also be seen from the figure.

Figure 11. The free surface at three different positions
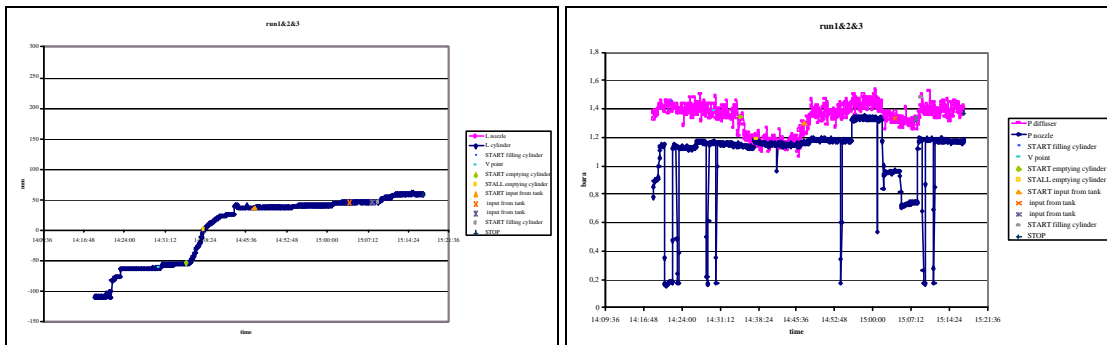
Figure 12. Effects of adding and removing Hg to and from the loop on Hg level and pressures

It was concluded from these experiments that the more slender nozzle DG16.5 has the desired potential. The absence of cavitation allows us to position the free surface arbitrarily by adding or removing Hg to/from the loop. A conical shaped flow pattern with a reduced re-circulation zone at the centre can be obtained. The conical flow has a velocity of about 2,5 m/s and is expected to be capable of removing the heat deposited by the proton beam (according to CFD calculations).

Below a certain value for the level, droplet spitting occurs. This is of course to be avoided as the droplet might evaporate and jeopardise the vacuum of the beam line. In the future, we will estimate to which extent (if at all) droplet formation can be tolerated. An optimisation process needs to be carried out to minimise the formation. One should also mention that due to a difference in surface tension, the behaviour of Hg and Pb-Bi with respect to the droplet formation will probably be different and – backed by some indicative and qualitative experience in other laboratories - it is expected that the formation will be lower for Pb-Bi.

IV. Supporting CFD Simulations

In parallel with the experiments, numerical simulations using CFD codes are performed aimed at reproducing the existing experimental results and giving input for the optimisation of the head geometry in the experiments. This paper describes the simulations in support of the Hg experiments. Other calculations were already reported (Van Tichelen, 2000). All reported simulations are performed using the VOF-mode of the FLOW-3D code (Hirt, 1981).

First CFD calculations were performed for the nozzle DG33.0 in order to evaluate its performance before experimenting. In the first instance, the cavitation model was not used. This lead to the unphysical results shown in Fig. 13. A zone with large negative pressures occurs at the entrance of the central tube. As the region above the free surface was fixed to zero pressure because of the vacuum, these negative pressures are not physical. Correspondingly, a very large acceleration of the fluid takes places in this zone.

These unphysical results led to believe that cavitation would occur in the nozzle at these very places. An indication for correctness of this conclusion was found when the cavitation model was turned on. The results are given in Fig. 14. One clearly sees the fluid detaching from the wall at the entrance of the central tube. A zero pressure cavitation region is formed. The exact appearance and extent of this region can however not be predicted by the code. Referring to § II.III.III., the effect of 'backfilling' is the reduction of the cavitating region by inserting Hg. In this way, the region can be reduced to the extent that the liquid only falls over a small distance such that the force behind the liquid returning to the wall is limited. We would also expect that later on to have only limited effect on the damaging the structural materials; hence our strict definition of cavitation at this stage.

The results also show that – due to the zero pressure cavitation region – there is a physical de-coupling between the lower pressure boundary and the free surface dome by a zero pressure region. Reducing the height of the dome by decreasing the outlet pressure is not possible. Moreover, the high radial velocity component makes that a high dome can be supported. This was confirmed by the experiments albeit the appearance of the dome in experiment and CFD simulation does not match.
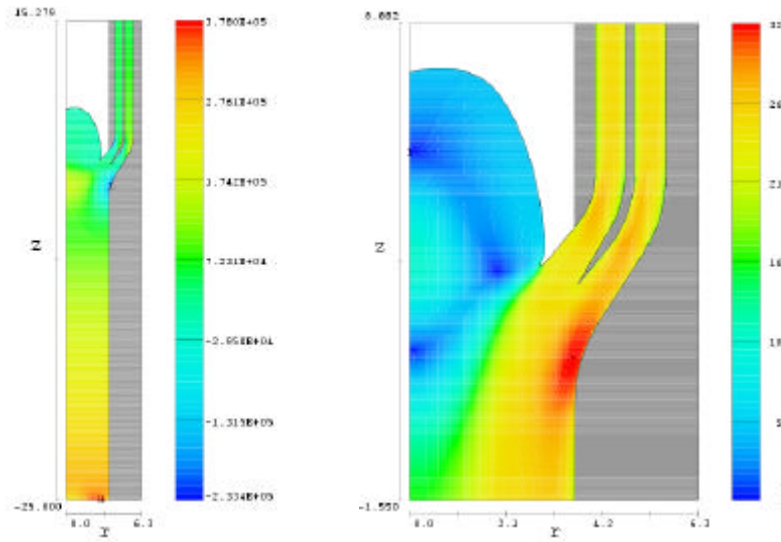
Figure 13. DG33.0: Pressure and velocity fields for the no-cavitation model (units: g-cm-s)
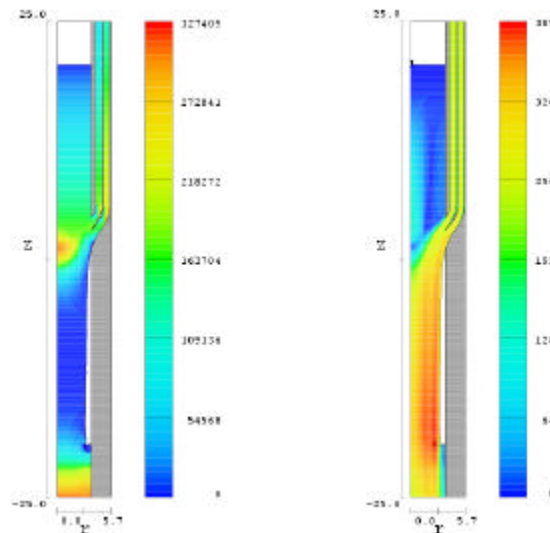
Figure 14. DG33.0: Pressure and velocity fields for the cavitation model (units: g-cm-s)
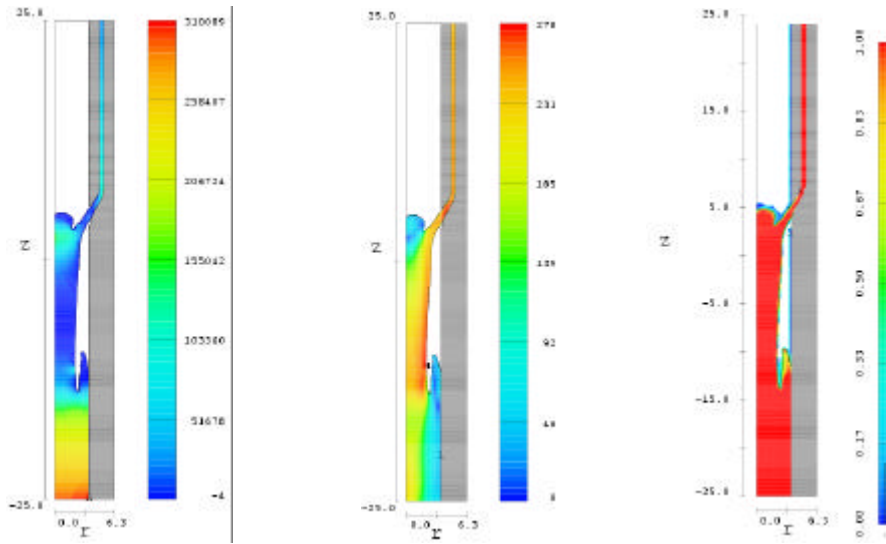
Figure 15. SG33.0: Pressure, velocity and fraction of fluid fields for the cavitation model (units: g-cm-s)

The same conclusions were arrived at retrospectively for the small gap nozzle SG33.0 (Fig. 15). The region of cavitation is even larger here due to the larger radial velocities. Again, the height of the dome could not be minimised.

For completeness, Fig. 15 shows a plot of the fraction of fluid in each grid cell. One can see that the surface is quite sharply tracked. However, when comparing to the experiments, the height of the fluid dome is overestimated in most of the cases. Therefore, in general, the velocity distributions are not to be believed at the free surface region.

The need for a smaller entrance angle became clear from the experiments and calculations. An angle of 16.5° was chosen and the flow for this nozzle was simulated - first using the non-cavitation model. The free surface region and the pressure outlet are then coupled and a reduction of the lower pressure immediately lower the free surface. The position of the surface can be set arbitrarily by changing the lower boundary condition. Two results at two different surface positions are shown in Fig. 16. However, in both cases a negative pressure region is present at the central tube entrance – this indicates the possible presence of cavitation.
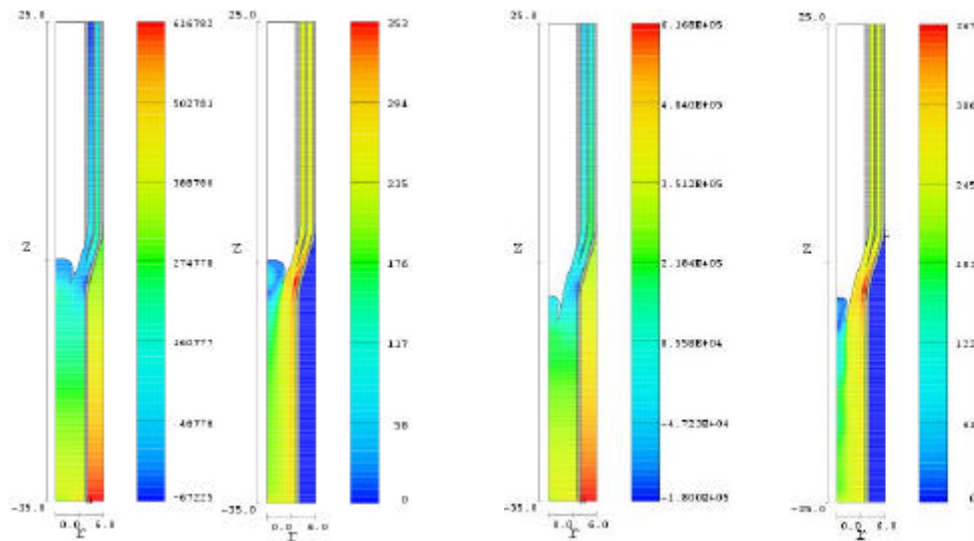
Figure 16. DG16.5: Pressure and velocity fields for the non-cavitation model at two free surface positions (units: g-cm-s)
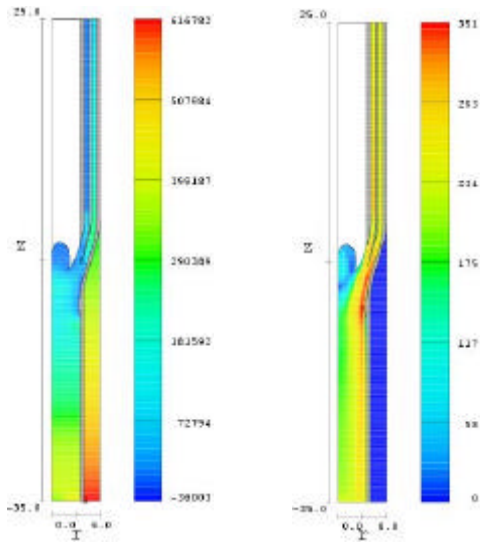
Figure 17. DG16.5: Pressure and velocity fields for the cavitation model at high free surface position (units: g-cm-s)

For the higher surface position, this negative pressure is small. It is therefore expected that cavitation will be limited and will not have a large influence on the free surface flow field. A preliminary calculation with cavitation points in this direction. The results are shown in Fig. 17. Moreover, due to the limited cavitation, there is still a coupling of the free surface region and the pressure outlet which might allow a further lowering of the free surface. This will be investigated in the near future.

For the lower free surface position, the negative pressure is larger. Therefore, switching on the cavitation model is expected to have a larger influence. A first indication can be found in the preliminary results with cavitation shown in Fig. 18. The cavitation region is larger but could possibly be reduced by backfilling as no significant cavitation is observed in the experiments. Splashing of the liquid occurs at the centre. It is to be investigated whether this is a numerical artefact – stemming from the fact that we permit only axi-symmetric solution - or whether it is a representation of the droplet spitting observed in the experiments. However, it is clear that only small amounts of liquid are shown to escape the main flow and have to be considered for the overheating problem.
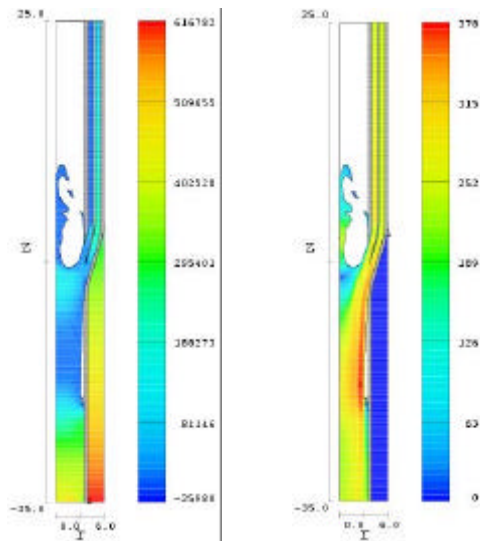
Figure 18. DG16.5: Pressure and velocity fields for the cavitation model at low free surface position (units: g-cm-s)

III. FUTURE STEPS

I. Optimisation Experiments with Water and Mercury

It can be concluded from § II.III.IV. that a smooth entrance angle is necessary to eliminate cavitation and to allow arbitrary positioning of the free surface. A smooth angle however reduces the available irradiation space. The angle of 16.5° was arbitrarily chosen so an optimisation program is necessary to determine the threshold angle of cavitation. FLOW-3D is being used for this optimisation as the balance of momentum is well conserved.

In order to assess the heat removal capabilities of the free surface flow, the velocities at the free surface must be well known. The current CFD codes are not able to predict these velocities in a way that is sufficiently reliable. Therefore, an elaborate measurement program is necessary.

Moreover, the CFD codes are not successful in describing the observed phenomenon of droplet spitting at the surface and can therefore not be used to optimise the nozzle to minimise this spitting. Again, an extensive experimental program is indispensable for fine-tuning and optimisation of the nozzle.

Because of their relative simplicity, water experiments are now reconsidered for this optimisation, however, this time under vacuum and at flow rates up to 10 l/s. Subsequently, the optimised nozzle will be tested in the mercury loop.

II. Pb-Bi Experiments with ENEA

The logically first Pb-Bi loop experiments are foreseen to be performed in the CHEOPE loop at around 300°C in collaboration with ENEA (Brasimone, Italy) in 2001/2 and joint design activities are under way. A to-scale model of the MYRRHA spallation target will be inserted in the CHEOPE experimental vessel together with a MHD pump, a configuration that will correspond to the minimum closed loop configuration of a MYRRHA like spallation circuit. That way the experimental set-up will be free of most of the possible interference by other components of a large loop.

III. Pb-Bi Experiments with FZK

As the spallation target design is a crucial point for the MYRRHA project, final confirmation experiments are foreseen to be performed with the eutectic LM at similar temperatures. In view of this, a collaboration with Forschungszentrum Karlsruhe (FZK, Germany) has been negotiated and design work is also underway, aiming at inserting a to-scale model of the MYRRHA spallation target similar to the one in Fig. 4 in their KALLA Pb-Bi loop. This large circuit will then have two free surfaces - the 2nd one on top of the main loop pump (sump pump type) – and will

so allow to perform experiments in a configuration closer resembling the later spallation loop. This will ultimately yield also data on loop control parameters and corrosion-like phenomena (cf. Sobolev, 2001).

IV. CONCLUSION

The design of the MYRRHA spallation is very challenging: a Pb-Bi flow pattern with a free surface needs to be established within the geometrical constraints, adequate to remove the very concentrated heat deposition of the proton beam so that the thermal and vacuum requirements are met. A number of the design activities have been and are being performed to study the flow behaviour and to obtain an adequate design. These design activities include both experiments and CFD calculations and their interaction. In summary, the results of these activities, although not yet totally conclusive, look very encouraging to yield the desired target configuration. Another effort at SCK·CEN, not gone into here, is dealing with the vacuum and accelerator compatibility of the configuration. (cf. also Sobolev 2001).

REFERENCES

Aït Abderrahim, H., Kupschus, P., Jongen, Y., Ternier, S., *MYRRHA, A Multipurpose Accelerator Driven System for R&D, First Step towards Waste Transmutation*, SCK•CEN, Mol, BLG 841 (2000).

Aït Abderrahim, H., Kupschus, P., Malambu, E., Aoust, Th., Benoit, Ph., Sobolev, V., Van Tichelen, K., Ariën, B., Vermeersch, F., Jongen, Y., Vandeplassche, D., *MYRRHA, A Multipurpose Accelerator Driven System for R&D*, this conference (2001).

Hirt, C.W., Nichols, B.D., *Volume of Fluid (VOF) Method for the Dynamics of Free Boundaries*, Journal of Computational Physics 39, 201 (1981).

Malambu, E., *Neutronic Performance Assessment of the MYRRHA ADS Facility*, SCK•CEN, Mol, R3438 (2000).

Seynhaeve, J.-M., Winckelmans, G., Bolle, L., Jeanmart, H., *MYRRHA project: R&D Collaboration between SCK•CEN and UCL/TERM: Phase 1 and 2*, Université Catholique de Louvain, Louvain-la-Neuve (2000).

Seynhaeve, J.-M., *MYRRHA project: R&D Collaboration between SCK•CEN and UCL/TERM: Phase 3*, Université Catholique de Louvain, Louvain-la-Neuve (2000).

Sobolev, V., Van Dyck, S., Kupschus, P., Aït Abderrahim, H., *Researches on Corrosion Mitigation in MYRRHA multipurpose ADS for R&D*, this conference (2001).

Van Tichelen K., Kupschus P., Aït Abderrahim H., Seynhaeve J.-M., Winckelmans G., Jeanmart H., Roelofs F., Komen E., MYRRHA: Design of a Windowless Spallation Target for a Prototype ADS, Proc. Ofthe 10th Int. Conf. Emerging Nuclear Energy Systems, Petten (2000).